J Nanostruct 13(2): 341-352, Spring 2023

RESEARCH PAPER

# Stable Perovskite Solar Cells Resist to Water without Encapsulation by P-Type Si Nws as Hole Collection Layers

*Karwan M. Rahman [1], Omid Amiri [2]*,Karim A. Younis [1], Muhammad H. Khalil [1], Amir Mahyar-Azhdarpor [3], Mohsen Saadat [4], Mohahmad A. Jamal [5], Nabaz A. Abdulrahman [5], Savana J. Ismael [1], Kuestan A. Ibrahim [1], and Sangar S. Ahmed [1]*

[1] *Chemistry Department, College of Science, Salahaddin University, Kirkuk Road, 44001, Erbil, Kurdistan Region, Iraq*

[2] *Chemistry Department, College of Science, University of Raparin, Rania, Kurdistan Region, Iraq*

[3] *Applied Geological Research Center of Iran, Karaj, Iran*

[4] *Department of Physics, University of Sistan and Baluchestan, Zahedan, Iran*

[5] *Department of Petroleum and Mining Engineering, Faculty of Engineering, Tishk International University, Erbil, Iraq*

**ARTICLE INFO**

***Article History:***
*Received 10 January 2023*
*Accepted 28 March 2023*
*Published 01 April 2023*

***Keywords:***
*Hole Transporting Material*
*Perovskite solar cell*
*Stability*

**ABSTRACT**

In the present work we introduce p-type Si Nano wires (Si NWS) as a hole transport material. As is well known, $CH_3NH_3PbI_3$ are extremely sensitive to moisture in air but p-type Si Nano wires could protect it from moisture and water. Highly stable $CH_3NH_3PbI_3$ perovskite absorber with the grain size up to 2 µm was prepared by dip coating method. The cell based on this stable perovskite absorber film achieves a high power conversion efficiency of 21.1%. $CH_3NH_3PbI_3$ perovskite absorber shows very high stability, it even was stable after washing with water without any encapsulation. We believe that this great stability comes from our new hole $CH_3NH_3PbI_3$ materials. In this work p-type Si NWs are used as HTM which lead to stabilized $CH_3NH_3PbI_3$ perovskite absorber even under direct flow of water. Degradation of $CH_3NH_3PbI_3$ perovskite absorber on mesoporous $TiO_2$ (it was deposited on $TiO_2$ by same method and condition) was studied to approve this hypothesis that stability comes from new HTM. $CH_3NH_3PbI_3$ perovskite absorber on mesoporous $TiO_2$ was completely degraded after 7 dayss while $CH_3NH_3PbI_3$ on Si NWs as HTM was quite stable for 50 days. This stability achieved whilst it was washed with water after 41 days (see video in supporting information). XRD and Pl were used to monitoring degradation of perovskite absorber layer over the time. The results provide an important facile approach to fabricate high-efficiency, stable and large area perovskite solar cell/module which accelerate the time to market.

**How to cite this article**
*Rahman K M., Amiri O., Younis K A. et al. Stable Perovskite Solar Cells Resist to Water without Encapsulation by P-Type Si Nws as Hole Collection Layers. J Nanostruct, 2023; 13(2):341-352. DOI: 10.22052/JNS.2023.02.003*

## INTRODUCTION

Perovskite solar cells only need 8 years to overcome barrier of dye sensitized solar cells (low efficiency) and its efficiency have increased from 3.8% in 2009 [1] to 22.7% in late 2017, [2] making this the fastest-advancing solar technology to date which its efficiency is comparable with silicon solar cells. That why perovskite solar cells became

* *Corresponding Author Email: o.amiri1@gmail.com*

a hot topic. According to the Web of Science Database 2294 articles related to the perovskite solar cell were published in 2016 and 4353 articles have published from 2015 to April 2017. Among perovskite materials with formula of $ABX_3$, the perovskite materials base on $CH_3NH_3PbI_3$ ($MAPbI_3$) has recently been identified as a promising absorber layer for solar cells because of high carrier mobility, long charge-carrier diffusion and high absorption coefficient [3]. Although perovskite solar cell overcomes efficiency limitation, it still suffers from instability.

Long-term device stability in the air atmosphere is the most persistent issue that delays perovskite solar cell commercialization [4-7]. The origin of this instability is perovskite absorber materials which were degraded in presence of water, oxygen and ultraviolet light. To date, most reports characterize device stability in the absence of these extrinsic factors [4-7]. Significant attention has been brought towards improving the stability of the devices but it still has remained challenging [4-7].

Current state of the arte strategy for stabile perovskite solar cells can be classified as four ways. First, improving stability by replacing MA cation with other cations. For instance Gratzel and et al. Replace MA with Cs and Fa which lead to improve stability [8]. According to their report, $FA_{0.9}Cs_{0.1}PbI_3$ film was stable for 19 h. In another report, Michael Saliba and Co-workers show that Cs $x(MA_{0.17}FA_{0.83)(1-x)}Pb_{(I0.83}Br_{0.17)3}$ film is stable for 250 h under operational conditions [9]. Second, adding additive in the perovskite solutions. Adding additive is another way to improve stability of perovskite solar cells. For example Zhao et al. fabricate perovskite solar cell with 300 h stability by adding polyethylene glycol (PEG) in the perovskite solution [10]. Grätzel and co-workers used phosphonic acid ammonium additives (4-ABPACl) forming the crosslinking of $CH_3NH_3PbI_3$ perovskite via strong hydrogen bonding of the $-PO(OH)_2$ and $-NH^{3+}$ [11] which shows better efficiency and stability. It was stable at 45 °C for one week. Third, inorganic HTM: using inorganic HTM is another way to improve stability of perovskite solar cells. Bian and co-workers introduced CuOx as HTL in the inverted planar p-i-n PVSCs,[12] in which the stability test of the unencapsulated device with $CuO_x$ flm suggested superior stability than that of device with PEDOT:PSS layer. In another research reported by J. You and et al. 1440 h stability with PCE of 16.1% was achieved by using NiOx as HTM [13]. In another report which was published in JACS, stability of 2h was achieved by using CuI as HTM [14]. Forth, encapsulation is last way to improve perovskite solar cells. For example Leijtens et al. demonstrated that the when $CH_3NH_3PbI_{3-x}Cl_x$ perovskite devices with a mesoporous $Al_2O_3$ scaffold were encapsulated with an epoxy resin and a glass coverslip in a nitrogen-filled glove box was stable for 1000 h [15]. Yong and co-workers introduced a hydrophobic polymer Teflon as polymer encapsulation to enhance stability of perovskite solar cell under ambient atmosphere conditions and 30 d stability was achieved [16]. The PVSCs also showed stable behaviour over a certain time while it was even immersed in water.

To solve this problem we need to protect absorber layer from these extrinsic factors. Using suitable hole-transporting materials (HTMs) could be a bright idea.

At present, state-of-the-art devices generally employ a p-type organic small-molecule or polymeric hole-conductor as hole-transporting layer (HTL), such as 2,2',7,-7'-tetrakis(N,N-di-p-methoxyphenylamine)-9,9'-spirobifluorene (spiro-OMeTAD) and poly(3- hexylthiophene) (P3HT) to achieve the highest efficiencies in perovskite solar cells [17- 19]. As mentioned previously, a critical limitation on commercializing this technology comes from its instability that could be solved by introducing suitable HTMs that offer full performance without sacrificing long-term stability, scalability, and with low material [20].

Since HTL forms the outer layer in typical perovskite solar cells, it is conceivable that the HTL could protect perovskite structure by shielding it from atmospheric moisture [19, 21-23]. The amount of this protection will consequently depend on the different parameters such as permeability, hydrophobicity and density of the hole-transporting material [19, 24-26]. These additional properties of the HTL could have a strong impact on the overall stability of this type of solar cells.

In the present work we introduce p-type Si Nano wires (Si NWS) as a hole transport material. As is well known, $CH_3NH_3PbI_3$ are extremely sensitive to moisture in air but p-type Si Nano wires could protect it from moisture. In fact we observe very high stability when Si NWS were used as HTM. Beside this Si NWS has some other advantages, Si has excellent hole mobility (2.34

× 109 T-2.7 cm2/Vs) which is much higher than Li doped spiro-MeOTAD (2 × 10-2 cm2/ V s ), its hole mobility almost 1011 times higher than spiro as common HTM for perovskite solar cells which is remarkable [27]. However, Si NWS have higher hole mobility compare to the Si wafer [28, 29]. Using Si NWS have some advantages compare to the Si wafer such as wider band gap, higher hole mobility and higher surface area. Definitely increasing band gap is the most important benefit of Si NWS which bring it up as an ideal HTM. Quantum confinement could increase bandgap of silicone to even 3 ev [30]. Our results shows that using silicon wafer with band gap of 1.1 ev drop of the efficiency to 7% while using Si NWS with band gap of 1.8 ev boost efficiency to 23.8 %. Currently, controlling environmental conditions to a moisture level of less than 1% is needed for device preparation because $CH_3NH_3PbI_3$ films are not stable in a humid atmosphere but in presence of Si NWS controlling environmental conditions is not needed [19, 31-33]. To be stable in air without the use of any type of encapsulation is an important factor for the operation of any device which Si NWS as HTM provide it. We even tested its water resistance and it was quite stable (See video and its XRD in supporting information). This is excited results which encourage researcher to use this new HTM in their future works.

## MATERIALS AND METHODS

### *Preparation of Si NWS*

P-type Si nanowires were prepared by wet chemical etching of silicon wafers. P-type single crystalline silicon with orientation (100) from Siltronic was employed as raw wafer. For all measurements, the samples were cut into 2×2 $cm^2$. Si wafers were cleaned by immersing in acetone, ethanol and HF (5 M) and DI water for 10 min respectively. The etching process was according to our previous work [34], briefly it was done in a sealed teflon vessel using a HF (5 M) and $AgNO_3$ (0.02 M) solution at 50 ℃.

### *$CH_3NH_3PbI_3$ coating*

In order to study the degradation of $CH_3NH_3PbI_3$, $CH_3NH_3PbI_3$ were coted on mesoporous $TiO_2$ (m-$TiO_2$) and Si NWs and their degradation were monitored by using XRD. In the case of $TiO_2$, First FTO glass was cleaned according to our previous work [35]. Briefly, it was sonicated by using ethanol, acetone and dried by nitrogen gun. Then compact layer of $TiO_2$ was coated by spin coating. Typically 1 mL of tetraethyl orthotitanate (TEOT) was dissolved in mixture of 1mL of $H_2O$, 1 mL HCl and 8 mL ethanol and was spin coated for 30 S with 2000 rpm. For coating m-$TiO_2$, $TiO_2$ paste purchased form Dyesol was diluted with ethanol (1:10 V:V) and spin coated for 45 S with 2000

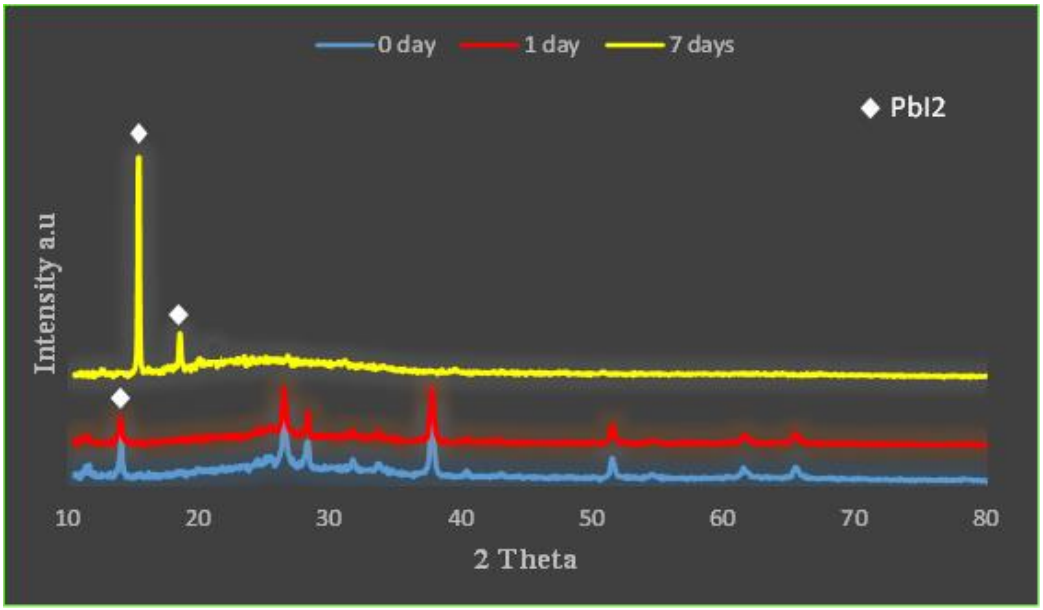


Fig. 1. Blue curve shows XRD pattern of fresh perovskite absorber layer on $TiO_2$ (a), red curve shows XRD pattern after 1 day (b), and yellow curve shows its XRD pattern after 7 days (c).

rpm. $CH_3NH_3PbI_3$ layer sequentially was deposited following procedures reported in paper 36. 0.4 M solution of $MAPbI_3$ perovskite were prepared by dissolving $PbI_2$ and $CH_3NH_3I$. It should be noted that all the solutions were then stirred for 1 h at 70 °C prior to use. The FTO/$TiO_2$ substrates were next preheated at 180 ℃ and was removed from the hot plate, dipped into the solution and quickly pulled out. The perovskite crystallized on the heat substrate within 5 s as indicated by the colour change from yellow to dark black. Same procedure was used to deposited perovskite layer on the Si NWS. It should be notice that before coating perovskite layer on Si NWS, Si NWS was immersed in HF in order to remove $SiO_2$ from its surface.

*Monitoring degradation of perovskite layer*

Degradation of perovskite layers were tested in air for 50 days by using XRD and Pl. Also we tested the stability of perovskite layer on Si NWS under direct flow of water. Characterization of Perovskite Films: Morphological characterizations were performed by scanning electron microscope (SEM).

**RESULTS AND DISCUSSION**

In order to study the stability of as fabricated perovskite layer XRD and Pl was used. Degradation of $MAPbI_3$ on the m-$TiO_2$ was studied as reference (PVSK-ref). XRD of PVSK-ref is shown in Fig. 1 a-c. Powder diagrams were recorded right after the dipping and after 1,2, and 7 days. Fig. 1a shows the XRD pattern of fresh PVSK-ref. Results show that PVSK-ref start to degrade after 1 day (Fig. 1 b) and it almost degraded in 7 days (Fig. 1 c).

Thin films of $MAPbI_3$ were grown on a hot Si (100) NWs which was briefly dipped into a hot mixture of MAI and $PbI_2$. Then powder diagrams were recorded right after the dipping and after 1, 2, 3, 7 and 30 days. As seen, $MAPbI_3$ on P-type Si NWS shows superior stability. Stability of $MAPbI_3$ on Si NWS was studied for 50 days (PVSK-Si). Related XRD patterns are shown in Fig. 2 a-f. We observed interesting and unusual behaviour in the case of formation of $MAPbI_3$ on Si NWS.

Fig. 2 a shows the XRD pattern for fresh $MAPbI_3$ on Si NWS. At first, deposited perovskite films do not show significant peak, but in the end it shows strong peak at 2θ=14 corresponding to (110). Its orientation has changed over the time. Fresh perovskite shows amorphous structures (Fig. 2 a). After 1days, $MAPbI_3$ crystal start to form and orient along the (110) (Fig. 2 b). After 2 days, we observed unexpected results, crystal orient along the (202) (Fig. 2 c). Surprisingly we observe crystal orient again along (110) and (220) after 3 days (Fig. 2 d). After 7 days, crystal oriented mainly along (110) (Fig. 2 e). After 30 days, its crystal orientation

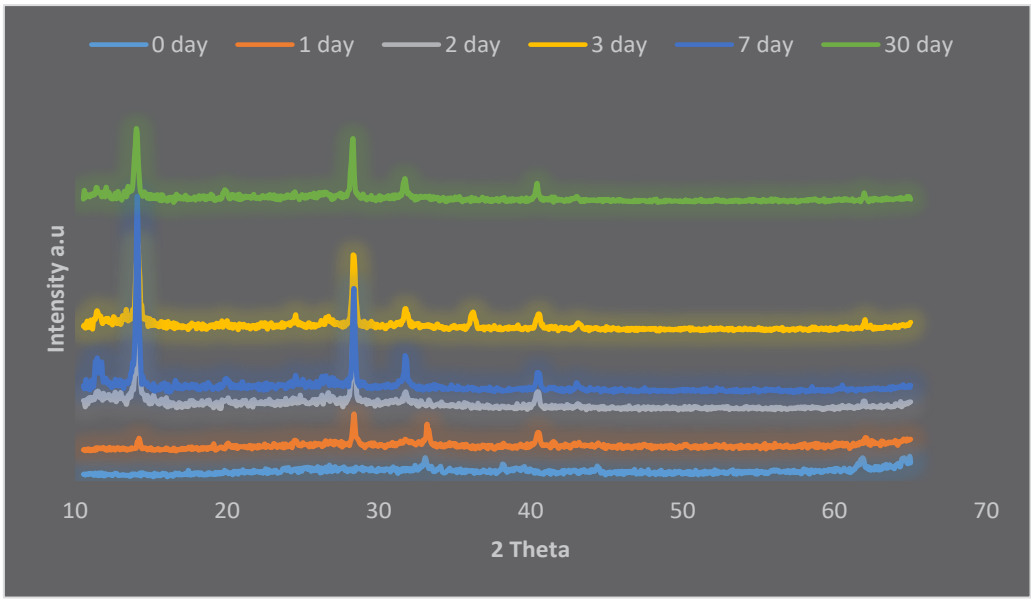


Fig. 2. XRD pattern of perovskite absorber layer on Si NWs: a) fresh sample, b) after 1 day, c) after 2 days, d) after 3 days, e) after 7 days, and f) after 30 days.

almost was same as 3 days (Fig.2. f). It seems this is smart crystal and continual oriented in different way to be stable against moisture on so on. This was strange results that why we repeated it and got same results (see XRD for repeated sample in supporting information, Fig. S1). In addition, we tested stability of perovskite layer on Si NWs under direct flow of water. For this, above sample (PVSK-Si) that its stability was studied for 42 days was chosen. After 43 days, it was placed under direct flow of water (see video in supporting information). Surprisingly it quit stable after washing with water. Related XRD patterns are shown in Fig. 3.

Fig. 3a and b show its XRD pattern after 1 day of washing with water and 6 days after washing, respectively. As seen from the figure, it quite stable even after washing with water and after 50 days after preparation. Briefly, since the first diagram shows a hardly crystalline simple, we may conclude that the system was in a quite undetermined state then and that the crystallites were rather small, especially since the sample underwent the cubic → tetragonal phase transition. The subsequent diagrams show the growth of the $MAPbI_3$ phase; this growth manifested in varying ratios of the $MAPbI_3$ lines. After about two days, an unknown

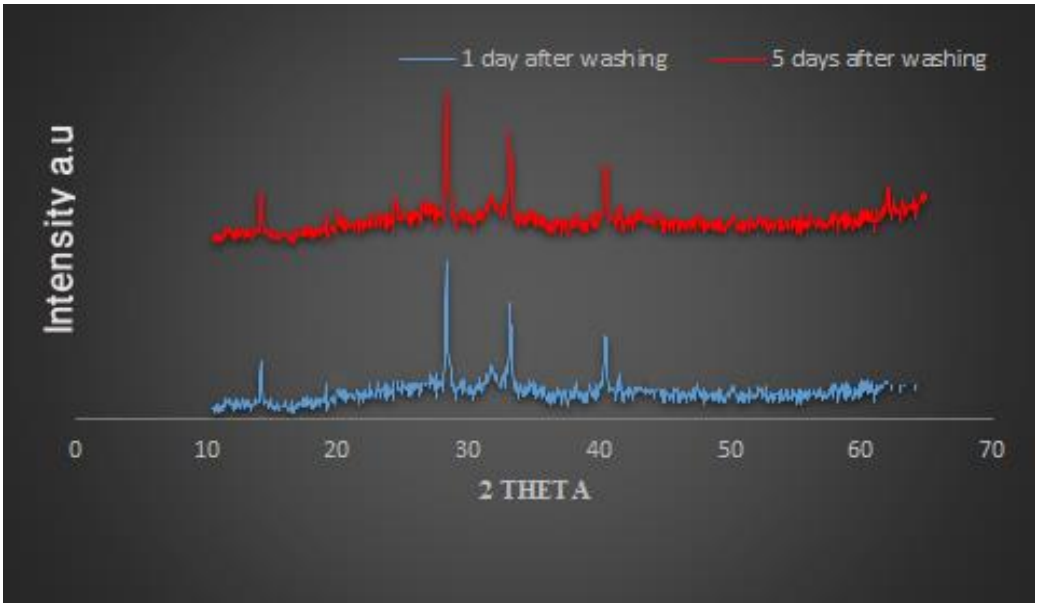


Fig. 3. XRD pattern of sample that prepared 41 days ago and then washed with water: a) after 1 day and b after 8 days.

Table 1. comparison between stability of various perovskite solar cells.

| stabilization method | | PCE | Stability | Ref. |
|---|---|---|---|---|
| Replacing A cation | Using FA0.9Cs0.1 | 17 | 19h in humidly | 8 |
| Replacing A cation | Using Csx(MA0.17FA0.83)(1−x) | 21.1 | 250 h in humidly | 9 |
| Adding additive | PEG | 16 | 300 h humidly | 10 |
| Adding additive | 4-ABPACl | 16.7 | 7 days humidly | 11 |
| Encapsulation | epoxy resin and a glass coverslip | | 1000 h in nitrogen atmosphere | 15 |
| Encapsulation | Teflon | 12 | 3 days under ambient atmosphere * | 16 |
| Inorganic HTM | CuOx | 17.1 | 250 h | 12 |
| Inorganic HTM | NiOx | 16.1 | 1440 h | 13 |
| Present work | p-Si NWs | 21 | 50 days | |

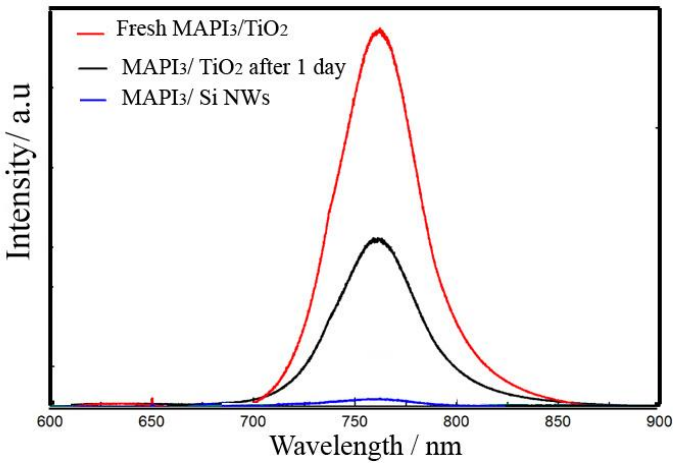


Fig. 4. Pl results for: a) fresh $TiO_2$/MAPbI3 film, b) after 1 day, c) $MAP_3$/Si NWs.

phase appeared which could not be identified, at least not in the C, H, N, I, Pb system.

This phase later disappeared and so we can say that the stable target $(CH_3NH_3)PbI_3$ was successfully produced. The stability of the presented perovskite could be compared with state of the art devices in term of stability (Table 1). Table 1 shows that all other reports without encapsulation were stable in humidly environmental while our device is stable under flow of water without any encapsulation.

Fig. 4a-b shows the PL results for $TiO_2$/$MAPbI_3$ film, PL intensity decrease over the time. We also use PL technic to demonstrate that Si NWS can extract holes. As seen from Fig. 4 c, PL of $MAPbI_3$ on Si NWS has low intensity because hole extracted from perovskite layer.

SEM and X-ray map were used to study the morphology and structure of Si NWS and perovskite layer. SEM results in Fig. 5 show that Si NWS have 60 nm diameters. $MAPbI_3$ crystal has about 2 µm grain size. EDX elemental maps showing well-defined layers and good infiltration

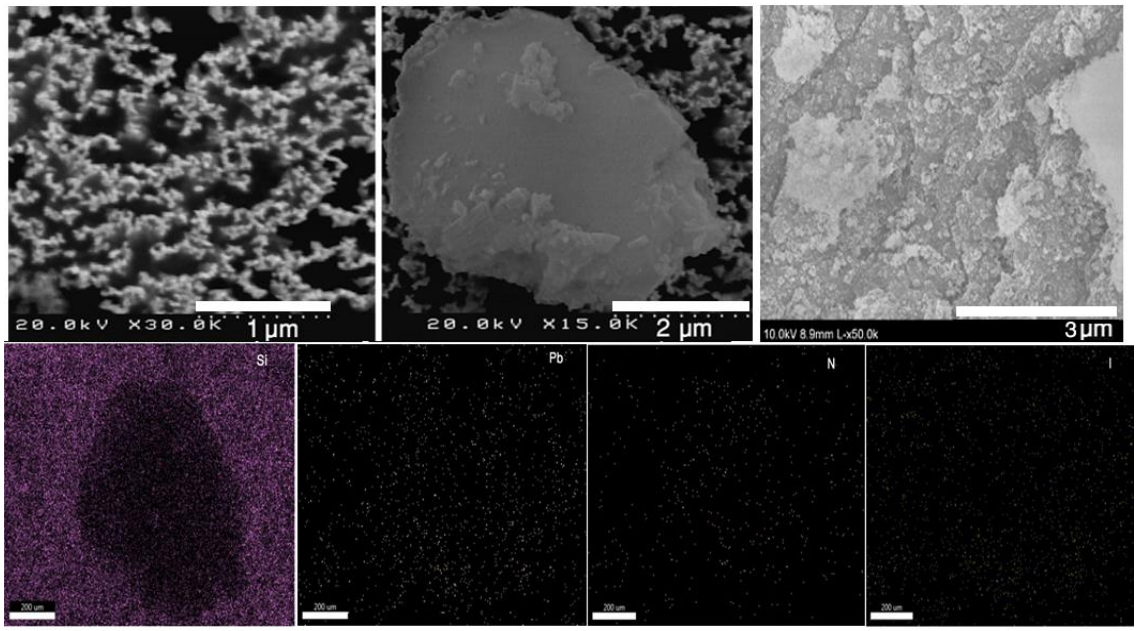


Fig. 5. SEM images of: a) bare Si NWs and b) SEM images of perovskite absorber layer on Si NWs and related EDX map.

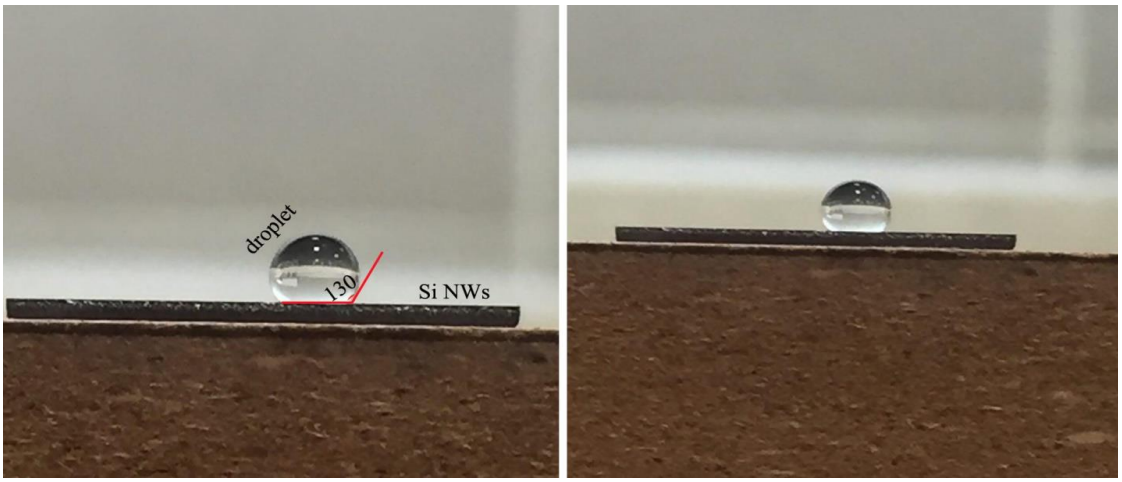


Fig. 6. Shows contact angel images for Si NWs.

of lead and iodine inside Si NWS.

We propose three possible reasons for unusual stability of perovskite layer on Si NWS: first, hydrophobic properties of Si NWS. Si NWS has hydrophobic properties that repel water from its surface. Therefore water or moisture could not reach the surface of Si and therefore protect perovskite layer from water. Fig. 6 shows contact angel images for Si NWs. Its contact angel is about 130 degree which confirms its hydrophobic properties. Second, orientation of perovskite crystals changed over the time (this may happens to be stable against moisture). Third, as seen from the XRD results, perovskite crystals form very slowly on Si NWS (it forms after 1 day). We are thinking that slow formation of crystal lead to slow down the degradation rate of perovskite. We will discuss last two reasons in our future work.

In this work, SCAPS version 3.2.01(a Solar Cell Capacitance Simulator) software which is a one dimensional solar cell simulation program is used to simulate perovskite solar cells. This software is developed at Department of Electronics and Information Systems (ELIS) of the University Of

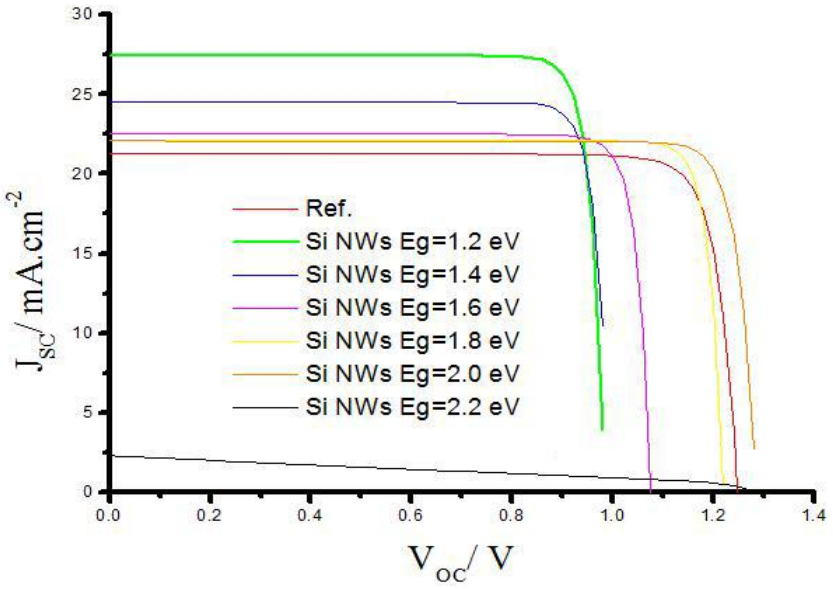


Fig. 7. Show I-V results for reference cell and cells with different Si NWs as HTMs.

Table 2. Solar cell parameters deduced from IV-curve.

| Cell | Voc/ V | Jsc /mA.Cm$^{-2}$) | FF | η |
|---|---|---|---|---|
| Ref. | 1.2 | 20.31 | 0.79 | 20 |
| Si NWs (100 nm)* | 0.89 | 22.57 | 0.31 | 6.32 |
| Si NWs (40-60nm) | 0.98 | 23.11 | 0.80 | 21 |
| Si NWs (7-10 nm) | 0.99 | 22.52 | 0.80 | 19.1 |
| Si NWs (5-7 nm) | 1.07 | 21.2 | 0.80 | 19.3 |
| Si NWs (3-5 nm) | 1.22 | 22.14 | 0.80 | 21.41 |

Gent, Belgium [36]. The simulated Perovskite solar cell has layer configuration with transparent conductive oxide (TCO)/ blocking layer ($TiO_2$)/ absorber/ and Si NWS as hole transport material. The considered materials for the mentioned layers are fluorine doped $SnO_2$ ($SnO_2$:F), pure $TiO_2$ , $CH_3NH_3PbI_3$ and spiro-OMeTAD (for reference cell), respectively. The thicknesses of layers are chosen based on experimental works on Perovskite solar cell [37]. To consider interface recombination, the interface layers INT1 and INT2 were defined from reference [38].

In this study, to obtain carrier diffusion lengths (Ln and Lp) of 1 µm that is similar to that of for experimental work [41], the value of defect parameters for all layers are considered identical and defect density for absorber is assumed equal to Nt= 2.5 × 1013 cm$^3$ [39].

Fig. 7 show I-V results for reference cell and cells with different Si NWs as HTMs. Also other important parameters are summarized at Table 2. From the results, reference cell shows efficiency of 20% VOC = 1.24 V, FF= 0.79, and JSC = 20.31 mA.cm$^{-2}$, respectively. When we used Si NWs with band gap of 1.1 ev which is equal to those in balk, efficiency, VOC, FF, and JSC dropped to 6.32 %,

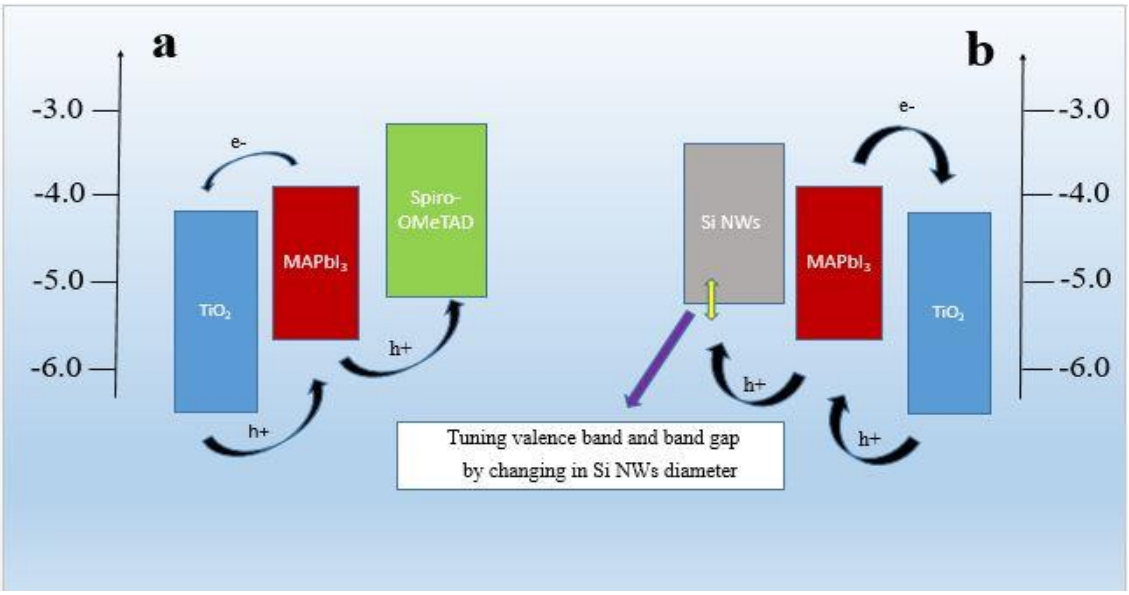


Fig. 8. Related band diagram of perovskite solar cell based on Si NWs as HTM. As seen from the schematic, it is possible to tuning valance band and band gap of Si NWs by changing diameter of nanowires.

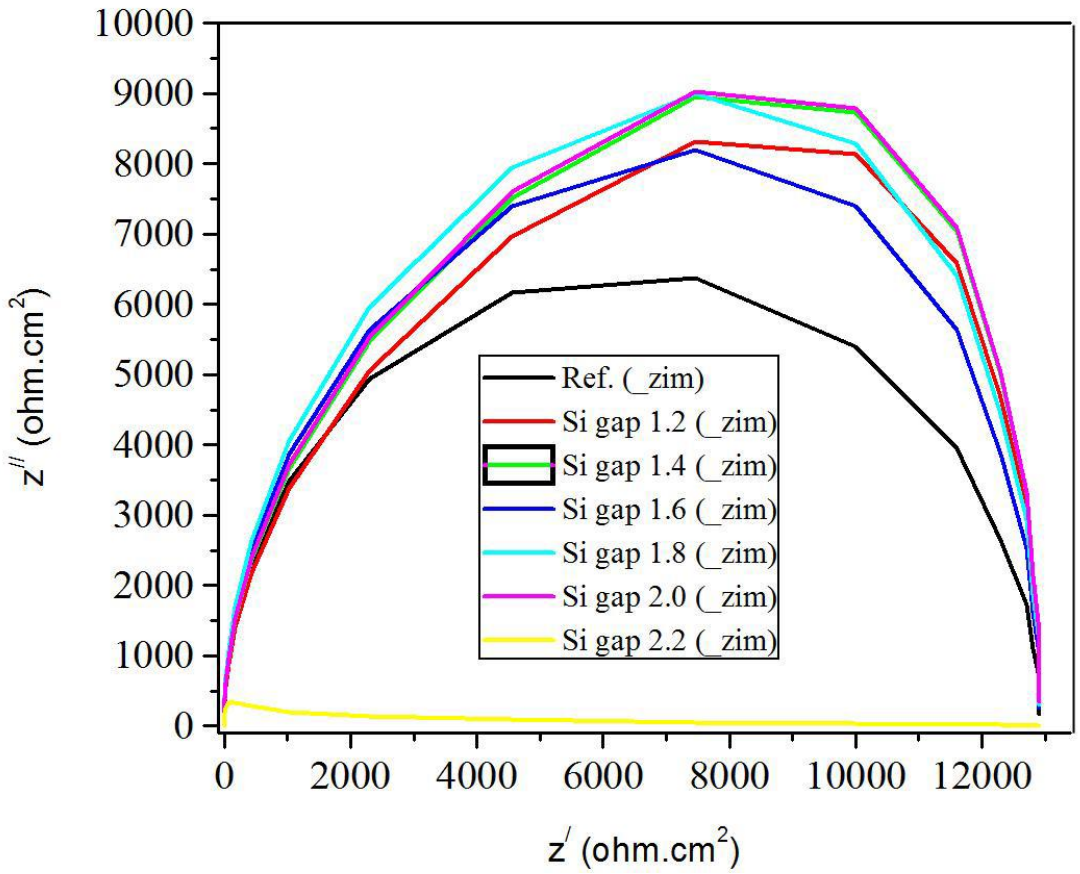


Fig. 10. Incident photon to converted electron (IPCE) results.

0.91 V, 0.30, and 22.57 mA.cm$^{-2}$, respectively.

By decreasing diameter of Si NWs, their band gap increased because of quantum confinement effect. As seen from the results, first, efficiency shows direct relation with increasing band gaps. When p-type Si NWs with band gap (60 nm in diameter) of 1.2 ev are used, efficiency of 21% are achieved. This cell has VOC, FF, JSC equal to 0.98 V, 0.80, and 23.11, respectively. Efficiency of 21.41 % is achieved when Si NWs with diameter of 5-7 nm was used. According to the P R Bandaru reports, its band gap is 1.4 ev [39].

As seen from the results, increasing band gap to 1.4 lead to decrease efficiency and JSC. By decreasing the diameter to 4 nm; consequently, band gap increase to 1.6 ev. In this case, efficiency, VOC, FF, JSC of 19.35 %, 1.07 V, 0.80, 21.20 mA.cm$^{-2}$, respectively. Optimum band gap is 1.8 ev which is achieved by Si NWs with diameter of about 4 nm. For this cell, related parameters are 21.1 %, 1.22 V, 0.89 and 22.14 mA.cm-2 for efficiency, VOC, FF, JSC, respectively. It seems that valence band of Si NWs determine efficiency. Fig. 8 shows related band diagram. As seen from the schematic, it is possible to tuning valance band and band gap of Si NWs by changing diameter of nanowires. Solar cells show better performance when valance band of Si NWs get closer to valance band of perovskite layer.

Electrical impedance spectroscopy (EIS) was adopted to evaluate charge transport and recombination in Si NWs based perovskite devices. Nyquist plot of these devices measured under dark with a 0.9 V bias is shown in Fig. 9. According to the equivalent circuit R1 indicate a series resistance, R2 interfacial resistance and R3 a recombination resistance, respectively.

Incident photon to converted electron (IPCE) results is presented in Fig. 10. Devices based on Si NWs with band gap of 2.2 ev show IPCE of less than 5 %. That why JSc of 2.5 mA.cm-2 was achieved for this cell. In other hand devices based on Si NWs

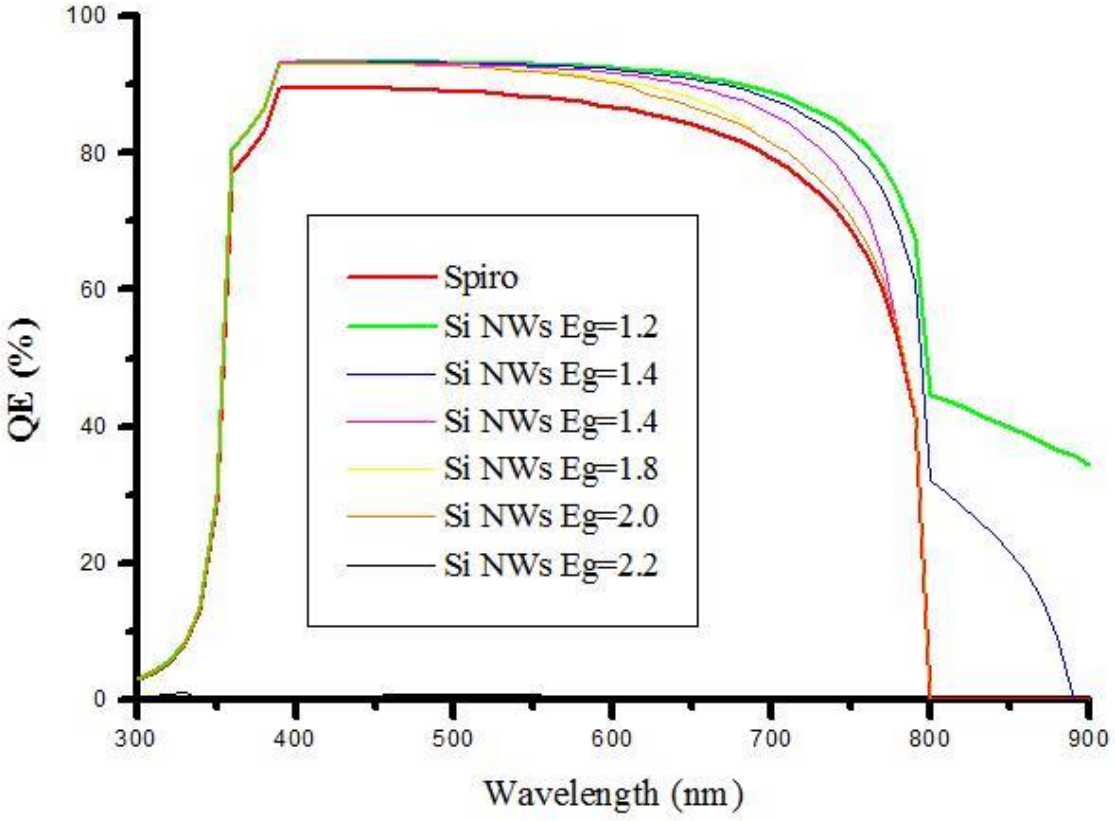


Fig. 10. Incident photon to converted electron (IPCE) results.

with band gap of 1.2 ev shows highest incident photon to converted electron ratio. Almost 90% of incident photon with wavelength between 400-700 nm converted to electron and hole pairs. For reference cell, this ratio is about 85% for same region

Our data shows that the series resistance almost is similar for all devices. Reference cell shows the lowest interfacial resistance while cell based on Si NWs with band gap of 1.8 ev shows highest recombination resistance. The larger interfacial resistance suggests that the Si NWs/ $MAPbI_3$ interface is less efficient for charge transport. However, the larger recombination resistance of the Si NWs based suggests that the perovskite active layer is more efficient at suppress charge recombination, consequently enhanced device photovoltaic performance [39].

## CONCLUSION

In conclusion, we report a new hole-transporting material (P-type Si NWs) to improve the stability of $MAPbI_3$ film under ambient atmosphere and flow of water. $MAPbI_3$ layer with was deposited on Si NWs with dip-coating method with grain size up to 3 µm and its degradation was monitored for 50 days. The champion p-i-n cell realizes very high stability even under water without any encapsulation. Our results shows that beside superior stability, it could exhibit very high efficiency exceed 21 %. The results provide an important facile approach to fabricate high-efficiency, stable and large area perovskite solar cell/module which accelerate the time to market. We propose three possible reasons for unusual stability of perovskite layer on Si NWS: first, hydrophobic properties of Si NWS. Si NWS has hydrophobic properties that repel water from its surface. Therefore water or moisture could not reach the surface of Si and therefore protect perovskite layer from water (contact angel for Si NWs is about 130 degree). Second, orientation of perovskite crystals changed over the time (this may happens to be stable against moisture) that why we named it, smart absorber layer. Third, as seen from the XRD results, perovskite crystals form very slowly on Si NWs (after 1 day).

## ACKNOWLEDGMENT

This work was supported by kashan university, for supporting this work. The authors want to thank Dr. Ahmad Amiri from Tehran University for the helpful discussions.

## CONFLICT OF INTEREST

The authors declare that there is no conflict of interests regarding the publication of this manuscript.

## REFERENCES

1. Kojima A, Teshima K, Shirai Y, Miyasaka T. Organometal Halide Perovskites as Visible-Light Sensitizers for Photovoltaic Cells. Journal of the American Chemical Society. 2009;131(17):6050-6051.
2. Yang WS, Park B-W, Jung EH, Jeon NJ, Kim YC, Lee DU, et al. Iodide management in formamidinium-lead-halide–based perovskite layers for efficient solar cells. Science. 2017;356(6345):1376-1379.
3. Smith IC, Hoke ET, Solis-Ibarra D, McGehee MD, Karunadasa HI. A Layered Hybrid Perovskite Solar-Cell Absorber with Enhanced Moisture Stability. Angew Chem Int Ed. 2014;53(42):11232-11235.
4. Christians JA, Schulz P, Tinkham JS, Schloemer TH, Harvey SP, Tremolet de Villers BJ, et al. Tailored interfaces of unencapsulated perovskite solar cells for >1,000 hour operational stability. Nature Energy. 2018;3(1):68-74.
5. Arora N, Dar MI, Hinderhofer A, Pellet N, Schreiber F, Zakeeruddin SM, et al. Perovskite solar cells with CuSCN hole extraction layers yield stabilized efficiencies greater than 20%. Science. 2017;358(6364):768-771.
6. Niu G, Li W, Meng F, Wang L, Dong H, Qiu Y. Study on the stability of CH3NH3PbI3 films and the effect of post-modification by aluminum oxide in all-solid-state hybrid solar cells. J Mater Chem A. 2014;2(3):705-710.
7. Liu J, Wu Y, Qin C, Yang X, Yasuda T, Islam A, et al. A dopant-free hole-transporting material for efficient and stable perovskite solar cells. Energy Environ Sci. 2014;7(9):2963-2967.
8. Yi C, Luo J, Meloni S, Boziki A, Ashari-Astani N, Grätzel C, et al. Entropic stabilization of mixed A-cation ABX3 metal halide perovskites for high performance perovskite solar cells. Energy & Environmental Science. 2016;9(2):656-662.
9. Saliba M, Matsui T, Seo J-Y, Domanski K, Correa-Baena J-P, Nazeeruddin MK, et al. Cesium-containing triple cation perovskite solar cells: improved stability, reproducibility and high efficiency. Energy & Environmental Science. 2016;9(6):1989-1997.
10. Zhao Y, Wei J, Li H, Yan Y, Zhou W, Yu D, et al. A polymer scaffold for self-healing perovskite solar cells. Nature Communications. 2016;7(1).
11. Li X, Ibrahim Dar M, Yi C, Luo J, Tschumi M, Zakeeruddin SM, et al. Improved performance and stability of perovskite solar cells by crystal crosslinking with alkylphosphonic acid ω-ammonium chlorides. Nat Chem. 2015;7(9):703-711.
12. Sun W, Li Y, Ye S, Rao H, Yan W, Peng H, et al. High-performance inverted planar heterojunction perovskite solar cells based on a solution-processed CuOx hole transport layer. Nanoscale. 2016;8(20):10806-10813.
13. You J, Meng L, Song T-B, Guo T-F, Yang Y, Chang W-H, et al. Improved air stability of perovskite solar cells via solution-processed metal oxide transport layers. Nature Nanotechnology. 2015;11(1):75-81.
14. Christians JA, Fung RCM, Kamat PV. An Inorganic Hole Conductor for Organo-Lead Halide Perovskite Solar Cells. Improved Hole Conductivity with Copper Iodide. Journal of the American Chemical Society. 2013;136(2):758-764.
15. Hwang I, Jeong I, Lee J, Ko MJ, Yong K. Enhancing Stability of Perovskite Solar Cells to Moisture by the Facile Hydrophobic Passivation. ACS Applied Materials & Interfaces. 2015;7(31):17330-17336.
16. Habisreutinger SN, Leijtens T, Eperon GE, Stranks SD, Nicholas RJ, Snaith HJ. Carbon Nanotube/Polymer Composites as a Highly Stable Hole Collection Layer in Perovskite Solar Cells. Nano Lett. 2014;14(10):5561-5568.
17. Chiang C-H, Nazeeruddin MK, Grätzel M, Wu C-G. The synergistic effect of H2O and DMF towards stable and 20% efficiency inverted perovskite solar cells. Energy & Environmental Science. 2017;10(3):808-817.
18. Berhe TA, Su W-N, Chen C-H, Pan C-J, Cheng J-H, Chen H-M, et al. Organometal halide perovskite solar cells: degradation and stability. Energy & Environmental Science. 2016;9(2):323-356.
19. Hou Y, Du X, Scheiner S, McMeekin DP, Wang Z, Li N, et al. A generic interface to reduce the efficiency-stability-cost gap of perovskite solar cells. Science. 2017;358(6367):1192-1197.
20. Kim JH, Liang PW, Williams ST, Cho N, Chueh CC, Glaz MS, et al. High-Performance and Environmentally Stable Planar Heterojunction Perovskite Solar Cells Based on a Solution-Processed Copper-Doped Nickel Oxide Hole-Transporting Layer. Adv Mater. 2014;27(4):695-701.
21. Kim JH, Williams ST, Cho N, Chueh CC, Jen AKY. Enhanced Environmental Stability of Planar Heterojunction Perovskite Solar Cells Based on Blade-Coating. Advanced Energy Materials. 2014;5(4).
22. Leijtens T, Eperon GE, Noel NK, Habisreutinger SN, Petrozza A, Snaith HJ. Stability of Metal Halide Perovskite Solar Cells. Advanced Energy Materials. 2015;5(20).
23. Zhang F, Shi W, Luo J, Pellet N, Yi C, Li X, et al. Isomer-Pure Bis-PCBM-Assisted Crystal Engineering of Perovskite Solar Cells Showing Excellent Efficiency and Stability. Adv Mater. 2017;29(17).
24. Kaltenbrunner M, Adam G, Głowacki ED, Drack M, Schwödiauer R, Leonat L, et al. Flexible high power-per-weight perovskite solar cells with chromium oxide–metal contacts for improved stability in air. Nature Materials. 2015;14(10):1032-1039.
25. Hawash Z, Ono LK, Qi Y. Photovoltaics: Recent Advances in Spiro-MeOTAD Hole Transport Material and Its Applications in Organic–Inorganic Halide Perovskite Solar Cells (Adv. Mater. Interfaces 1/2018). Advanced Materials Interfaces. 2018;5(1).
26. Niquet Y-M, Delerue C, Krzeminski C. Effects of Strain on the Carrier Mobility in Silicon Nanowires. Nano Lett. 2012;12(7):3545-3550.
27. Gunawan O, Sekaric L, Majumdar A, Rooks M, Appenzeller J, Sleight JW, et al. Measurement of Carrier Mobility in Silicon Nanowires. Nano Lett. 2008;8(6):1566-1571.
28. Bandaru PR, Pichanusakorn P. An outline of the synthesis and properties of silicon nanowires. Semicond Sci Technol. 2010;25(2):024003.

29. Bella F, Griffini G, Correa-Baena J-P, Saracco G, Grätzel M, Hagfeldt A, et al. Improving efficiency and stability of perovskite solar cells with photocurable fluoropolymers. Science. 2016;354(6309):203-206.
30. Mei A, Li X, Liu L, Ku Z, Liu T, Rong Y, et al. A hole-conductor–free, fully printable mesoscopic perovskite solar cell with high stability. Science. 2014;345(6194):295-298.
31. Farangi M, Zahedifar M, Mozdianfard MR, Pakzamir MH. Effects of silicon nanowires length on solar cells photovoltaic properties. Appl Phys A. 2012;109(2):299-306.
32. Amiri O, Salavati-Niasari M, Bagheri S, Yousefi AT. Enhanced DSSCs efficiency via Cooperate co-absorbance (CdS QDs) and plasmonic core-shell nanoparticle (Ag@PVP). Sci Rep. 2016;6(1).
33. Liao HC, Guo P, Hsu CP, Lin M, Wang B, Zeng L, et al. Enhanced Efficiency of Hot-Cast Large-Area Planar Perovskite Solar Cells/Modules Having Controlled Chloride Incorporation. Advanced Energy Materials. 2016;7(8).
34. Simya OK, Mahaboobbatcha A, Balachander K. A comparative study on the performance of Kesterite based thin film solar cells using SCAPS simulation program. Superlattices Microstruct. 2015;82:248-261.
35. Dette C, Pérez-Osorio MA, Kley CS, Punke P, Patrick CE, Jacobson P, et al. $TiO_2$ Anatase with a Bandgap in the Visible Region. Nano Lett. 2014;14(11):6533-6538.
36. Yadav MK, Ghosh M, Biswas R, Raychaudhuri AK, Mookerjee A, Datta S. Band-gap variation in Mg- and Cd-doped ZnO nanostructures and molecular clusters. Physical Review B. 2007;76(19).
37. Zhou H, Chen Q, Li G, Luo S, Song T-b, Duan H-S, et al. Interface engineering of highly efficient perovskite solar cells. Science. 2014;345(6196):542-546.
38. Yella A, Heiniger L-P, Gao P, Nazeeruddin MK, Grätzel M. Nanocrystalline Rutile Electron Extraction Layer Enables Low-Temperature Solution Processed Perovskite Photovoltaics with 13.7% Efficiency. Nano Lett. 2014;14(5):2591-2596.
39. Yang L, Yan Y, Cai F, Li J, Wang T. Poly(9-vinylcarbazole) as a hole transport material for efficient and stable inverted planar heterojunction perovskite solar cells. Sol Energy Mater Sol Cells. 2017;163:210-217.